

Control structure design for the 6 DOF tractor-semitrailer example

Citation for published version (APA):

Wal, van de, M. M. J. (1995). *Control structure design for the 6 DOF tractor-semitrailer example: application of the Matlab Control Configuration Design toolbox*. (DCT rapporten; Vol. 1995.124). Technische Universiteit Eindhoven.

Document status and date:

Published: 01/01/1995

Document Version:

Publisher's PDF, also known as Version of Record (includes final page, issue and volume numbers)

Please check the document version of this publication:

- A submitted manuscript is the version of the article upon submission and before peer-review. There can be important differences between the submitted version and the official published version of record. People interested in the research are advised to contact the author for the final version of the publication, or visit the DOI to the publisher's website.
- The final author version and the galley proof are versions of the publication after peer review.
- The final published version features the final layout of the paper including the volume, issue and page numbers.

[Link to publication](#)

General rights

Copyright and moral rights for the publications made accessible in the public portal are retained by the authors and/or other copyright owners and it is a condition of accessing publications that users recognise and abide by the legal requirements associated with these rights.

- Users may download and print one copy of any publication from the public portal for the purpose of private study or research.
- You may not further distribute the material or use it for any profit-making activity or commercial gain
- You may freely distribute the URL identifying the publication in the public portal.

If the publication is distributed under the terms of Article 25fa of the Dutch Copyright Act, indicated by the "Taverne" license above, please follow below link for the End User Agreement:

www.tue.nl/taverne

Take down policy

If you believe that this document breaches copyright please contact us at:

openaccess@tue.nl

providing details and we will investigate your claim.

**Control Structure Design for the
6 DOF Tractor-Semitrailer Example**

Application of the Matlab
Control Configuration Design Toolbox

Marc van de Wal

WFW Report 95.124

M. M. J. VAN DE WAL
Faculty of Mechanical Engineering
Eindhoven University of Technology
March 1995

Control Structure Design
for the 6 DOF Tractor-Semitrailer Example
Application of the Matlab Control Configuration Design Toolbox

Marc van de Wal

March 1995

Contents

1	Introduction	2
2	Input Output Selection	5
2.1	Uncertainty Description	6
2.2	Results	9
2.3	Discussion	12
3	Control Configuration Selection	15
3.1	Results	17
3.2	Discussion	20
	Bibliography	21

Chapter 1

Introduction

The Control Structure Design (CSD) method suggested in [3] will be illustrated for an active suspension design problem. The 6 DOF tractor-semitrailer as proposed in [5, Chapter 5] will serve as an example, see Fig. 1.1. For this purpose, the Matlab Control Configuration Design (CCD) toolbox [4] will be used: The selection of measured and manipulated variables and the selection of a decentralized control configuration will successively be discussed. Controller design and closed-loop control system evaluation will not be performed at this stage.

Three actuators, placed between the axles and the tractor chassis and semitrailer chassis respectively, are proposed as candidate inputs u_1 , u_2 and u_3 . The nine variables below are suggested as candidate measurements:

- suspension deflections $y_1 - y_3$,
- axle accelerations $y_4 - y_6$,
- vertical accelerations of the chassis at the suspension attachments at the front and at the rear of the tractor y_7 , y_8 and at the rear of the semitrailer y_9 .

In order for CSD to be performed, a linear model of the system is needed. A state space description which is assumed to represent the main characteristics of the system, is the following:

$$\begin{aligned}\dot{x}(t) &= Ax(t) + B_u u(t) + B_w w(t) \\ y(t) &= Cx(t) + D_u u(t) + D_w w(t) \\ z(t) &= Ex(t) + F_u u(t) + F_w w(t)\end{aligned}\tag{1.1}$$

with x the state variables, w the excitation of the system by the road, and z the variables to be controlled, *i.e.*, dynamic tire forces, suspension deflections and rotational and vertical accelerations of both driver and cargo. For details on the state space description, the reader is referred to [5, Chapter 5 and Appendix A].

The CSD method implemented in the CCD toolbox requires control systems to be represented as in Fig. 1.2. For this reason, the relation between the inputs u and w , and the measurements

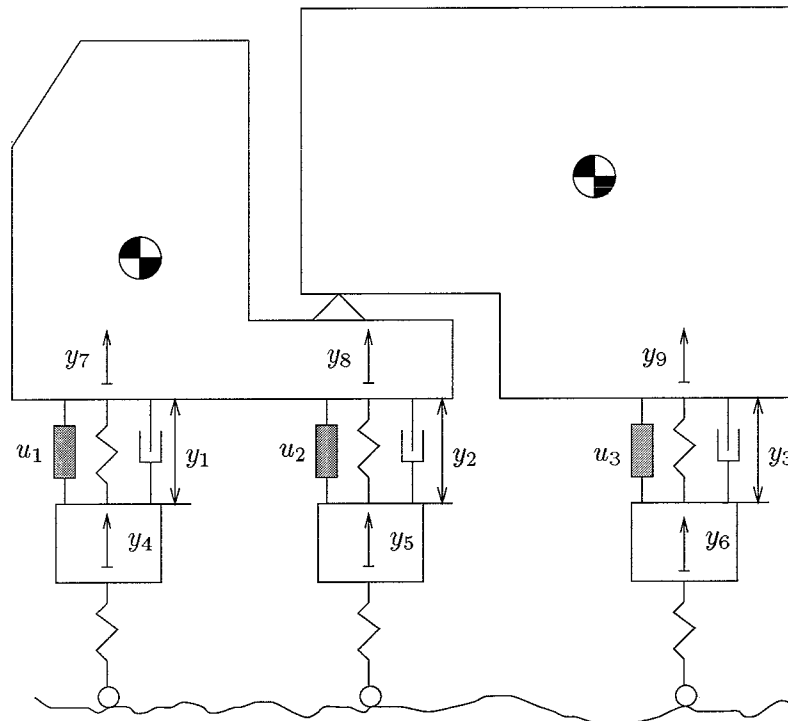
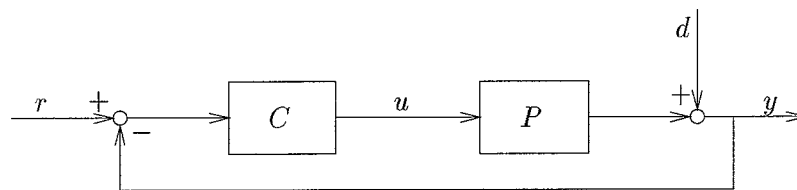


Figure 1.1: 6 DOF tractor-semitrailer model



- P : system to be controlled (plant)
- C : controller
- r : signals to be tracked
- d : disturbances
- u : manipulated variables (inputs)
- y : measured variables (outputs)

Figure 1.2: Control system set-up for the CCD toolbox

y in (1.1) is rewritten as follows:

$$y(s) = P(s)u(s) + d(s) \quad (1.2)$$

with:

$$\begin{aligned} P(s) &= C(sI - A)^{-1}B_u + D_u \\ d(s) &= (C(sI - A)^{-1}B_w + D_w)w(s). \end{aligned}$$

Here, the excitation by the road w is represented by disturbances d at the measured output y of the plant P .

A disadvantage of the particular CSD method is the prior assumption that the selected measurements y are strongly related to the variables to be controlled z , which need not be the same. This difference also occurs for the truck example, since the tire deflections must be kept within limitations, but cannot be measured directly. Under the assumption mentioned above, one tries to control z by means of controlling y . However, as will be discussed in Chapter 2, Input Output (IO) selection is based on robust stabilizability of the control loop in Fig. 1.2. As a consequence, an IO set may be selected for which the system is robustly stabilizable indeed, yet for which it cannot be controlled properly anymore. A criterion for *robust performance* is expected to suit better.

Since all modes of the tractor-semitrailer are stable, the system is both *stabilizable* and *detectable*. In fact, it can even be shown that the pair (C, A) is always *observable*, whatever subset of outputs y is selected, while the pair (A, B_u) is always *controllable*, whatever subset of inputs u is selected. Stabilizability and detectability are common requirements for successful design of output feedback controllers. For example, they are prerequisites for an \mathcal{H}_∞ - or μ -based controller design, which minimizes the ∞ -norm of the closed-loop transfer matrix between the external input w and the control error z of the system in (1.1) [1, Chapter 6]. If additional prerequisites for well-posedness in \mathcal{H}_∞ - or μ -based controller design are satisfied [1, Chapter 6], a measurement-based controller which minimizes the control errors in z can in principal be designed, whatever IO set is ultimately selected.

Chapter 2

Input Output Selection

The procedure for Input Output (IO) selection is summarized in [5, Section 3.9]. For the sake of completeness, the main result will be repeated here.

The fundamental idea for IO selection is maintenance of robust stabilizability of a control system under additive ∞ -norm bounded perturbations Δ , see Fig. 2.1. Note that stability does not depend on the presence of the disturbance signal d and the tracking signal r . The following theorem is proven in [3]:

Suppose P_0 is a square, Finite Dimensional Linear Time Invariant (FDLTI) nominal plant. Under these assumptions, there exists a FDLTI controller C which

1. stabilizes all $P = P_0 + \Delta$ with
 - (a) the same number of Right Half Plane (RHP) poles as P_0 and
 - (b) $\bar{\sigma}(\Delta)/\bar{\sigma}(P_0) \leq \delta_{ra}$, and
2. achieves $\bar{\sigma}(S) \leq \sigma_S$, $\sigma_S < 1 \forall \omega \leq \omega_S$

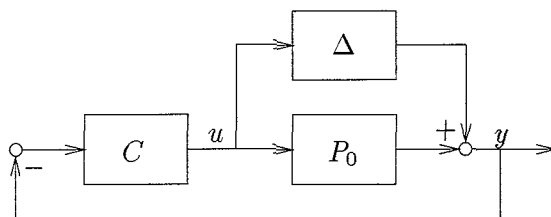


Figure 2.1: Additively perturbed control system

only if

$$\kappa(P_0) < \frac{1}{\delta_{ra}} \left(\frac{1}{1 - \sigma_S} \right) \forall \omega \leq \omega_S \quad (2.1)$$

where:

- $S = (I + P_0 C)^{-1}$ is the nominal output sensitivity function of the closed-loop system,
- $\kappa = \bar{\sigma}(P_0)/\underline{\sigma}(P_0)$ is the Euclidean condition number of the nominal plant,
- δ_{ra} is the specified, possibly frequency-dependent, relative additive uncertainty bound,
- σ_S and ω_S specify the closed-loop bandwidth of the system in terms of S .

It is emphasized that (2.1) is only a *necessary* condition for robust stabilizability (provision 1) together with a performance specification in terms of S (provision 2). Note that in the criterion above, which will be referred to as “Criterion 2” (as it is done in the software), the plant P corresponds to a *square subsystem* of the overall plant P^* , which is possibly non-square and incorporates all candidate measured and manipulated variables. For the particular example discussed here, the overall plant P^* has dimension 9×3 , while P is an $m \times m$ subsystem of P^* with $m \leq 3$. Candidate IO sets which do not satisfy criterion (2.1) are rejected.

Note that the condition number κ not only depends on the particular inputs and outputs under investigation, but also on their scalings. In [3], this gives rise to the development of a *scaling-independent* quantity, which is obtained from the so-called Relative Gain Array (RGA) Λ of the nominal plant P_0 : $\Lambda = P_0 .* (P_0^{-1})^T$, with $.*$ element-by-element multiplication. The motivation is however somewhat doubtful. In [3], it is remarked that “each time the plant is re-scaled, the condition number will have to be re-computed and the inequality re-evaluated”, which is time-consuming. However, once the overall system P_0^* is properly scaled, scaling need not be performed for each individual subsystem, since the scaled subsystem P_0 can be obtained by simply selecting the corresponding rows, columns and scaling coefficients from the overall system P_0^* . So, the introduction of the RGA-quantity as a way to make the IO selection less burdensome due to the need of re-scaling, seems questionable.

By substituting the “RGA quantity” $2 \max\{\|\Lambda(P_0)\|_1, \|\Lambda(P_0)\|_\infty\} - 1$ for $\kappa(P_0)$ in (2.1), the modified “Criterion 1” is created. Applying this criterion instead of Criterion 2, a larger number of IO sets will pass, since Criterion 1 weakens the necessary condition for robust stability. The selection procedure is less “severe”, since $2 \max\{\|\Lambda(P_0)\|_1, \|\Lambda(P_0)\|_\infty\} - 1 \leq \kappa(P_0)$. So, the IO selection may computationally be more *efficient*, though possibly *less effective*.

2.1 Uncertainty Description

In order to screen candidate IO sets by applying condition (2.1), an uncertainty bound δ_{ra} is needed. The criterion implies that for a specific choice of ω_S and σ_S a selected subset with

subsystem size	number of distinct subsystems
1	27
2	108
3	84
total:	219

Table 2.1: Number of distinct candidate IO sets

a large condition number can only tolerate small amounts of uncertainty without sacrificing stability. In the examples discussed in [3], δ_{ra} is purely used as a parameter to affect the number of IO sets passing the criterion. For example, if too large a number of IO sets passes (2.1) at a particular frequency ω , δ_{ra} is raised and additional IO sets are eliminated. However, it seems better to use a bound $\delta_{ra}(j\omega)$ on the *expected* uncertainty at each frequency. For example, it may be felt that there is hardly plant uncertainty at low frequencies, while there is a lot at intermediate and high frequencies.

By its definition, the relative additive uncertainty description δ_{ra} depends on the particular IO set selected. However, deriving an uncertainty bound for each IO set individually is infeasible for a large number of candidates. For this reason, an upper bound which accounts for uncertainties *for all candidate IO sets* will be derived. A fact is [3, Appendix A], that $\bar{\sigma}(P_0) \leq \bar{\sigma}(P_0^*)$, and $\bar{\sigma}(\Delta) \leq \bar{\sigma}(\Delta^*)$, with P_0 and Δ “subsystems” of the 9×3 “systems” P_0^* and Δ^* respectively. Unfortunately, *a priori* nothing meaningful can be said about the relation between $\bar{\sigma}(\Delta)/\bar{\sigma}(P_0)$ and $\bar{\sigma}(\Delta^*)/\bar{\sigma}(P_0^*)$. Instead, δ_{ra} must be obtained by computing relative additive error bounds for *all* candidate IO sets. Note that this may be infeasible for a highly dimensional P_0^* . In Table 2.1, the number of square IO sets which can be created from the overall 9×3 system is listed.

It is obvious that a lot of errors play a role in the system model. In practice, the difference between the linear model (1.1) and the real system arises from a variety of sources, *e.g.*, varying weight of the cargo, nonlinear and uncertain spring and damper characteristics and wrong inertia parameters. In [2, Section 6.2], it is stated that the damping coefficients of the suspension are hardly accurate. For this reason and the impossibility to account for all uncertainties, this investigation will be restricted to a 25% error in the three damper parameters simultaneously.

The uncertainty bound is now derived in the following way. Firstly, the relative additive uncertainties $\bar{\sigma}(\Delta)/\bar{\sigma}(P_0)$ are computed for all 219 candidate subsystems. It appears that the envelope for the magnitudes of the uncertainties for the 1×1 IO sets (obtained by taking at each frequency the maximum of the 27 relative additive uncertainty values) is greater than or equal to the envelope for the 2×2 IO sets, which in turn is greater than or equal to the one for the 3×3 IO sets, in the whole frequency range of interest, see Fig. 2.2.

In the following, σ_S is fixed at $\frac{1}{2}\sqrt{2}$ (as it is always done in [3]), *i.e.*, $\bar{\sigma}(S)$ is specified to lie below the -3dB level for all frequencies less than ω_S . If the uncertainty description were based on the envelope for the 1×1 IO sets, the right hand side of (2.1) would be larger than 1 for the whole frequency range of interest. Since the condition number of a 1×1 IO set equals one, all these candidates trivially pass the criterion and are therefore not further considered

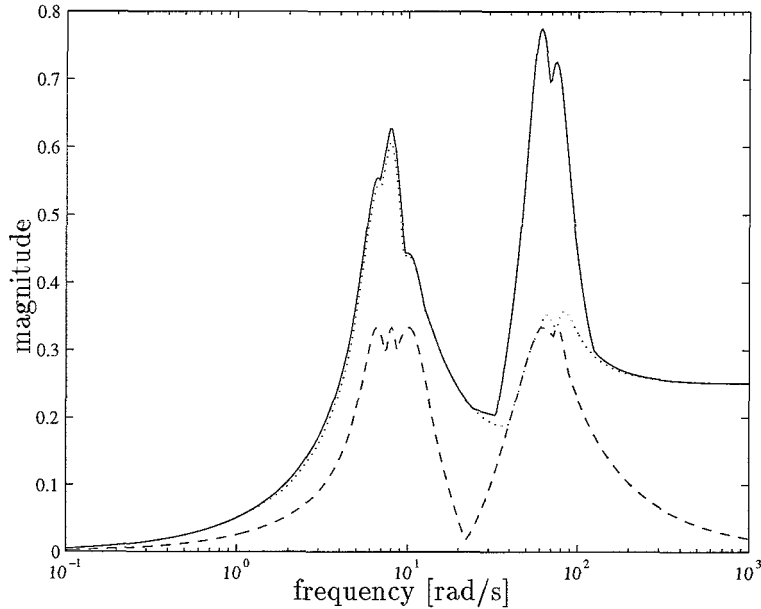


Figure 2.2: Maximum relative additive uncertainties for 1×1 (-), 2×2 (·), and 3×3 (- -) IO sets.

parameter	δ_{ra}
α	0.27
β	0.01
ζ_1	3.50
ζ_2	0.36
ω_c	0.72

Table 2.2: Parameters for relative additive uncertainty bound δ_{ra}

in this section. As a consequence, the derivation of δ_{ra} will only be based on the envelope for the combined 2×2 and 3×3 IO sets. This yields a less conservative uncertainty bound than in the case the 1×1 IO sets are also accounted for.

The bound which is used to represent the maximum relative additive uncertainties below ω_S is depicted in Fig. 2.3. It is obtained by taking the magnitude of the transfer function

$$\delta_{ra}(s) = \frac{\beta(\alpha s^2 + 2\zeta_1\omega_c\sqrt{\alpha}s + \omega_c^2)}{\beta s^2 + 2\zeta_2\omega_c\sqrt{\beta}s + \omega_c^2},$$

the parameters of which are listed in Table 2.2.

From Fig. 1.2 it can be seen that the closed-loop behavior between d and y is represented by the sensitivity S . In [2, Section 3.1], it is stated that vertical accelerations in the frequency range between 4 and 8 Hz are highly undesirable for good driver comfort. In order to attenuate undesirable frequencies in d , the bandwidth ω_S of S is specified as $2\pi \times 8 \approx 50$ rad/s.

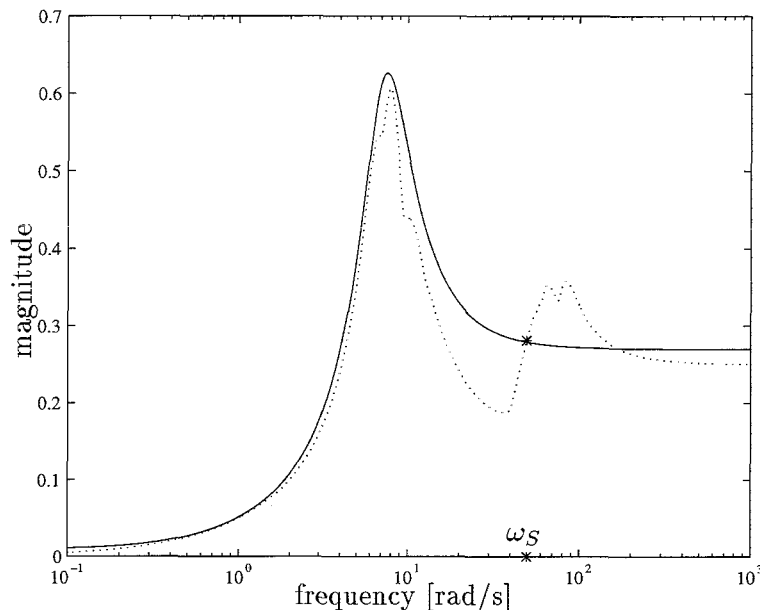


Figure 2.3: Maximum relative additive uncertainty for combined 2×2 & 3×3 IO sets (\cdots) and relative additive uncertainty bound ($-$)

2.2 Results

In this section, IO selection for the tractor-semitrailer will be performed. The difference in strength between Criterion 1 and Criterion 2 is illustrated for three candidate IO sets: $y_1 y_2 y_3 / u_1 u_2 u_3$, $y_1 y_3 y_4 / u_1 u_2 u_3$, and $y_1 y_3 y_5 / u_1 u_2 u_3$. In Fig. 2.4, the left hand side of (2.1) for Criterion 1 and Criterion 2 respectively, is compared with the evaluation bound $1/(\delta_{ra}(1 - \sigma_S))$. Application of Criterion 1 only eliminates $y_1 y_2 y_3 / u_1 u_2 u_3$, while Criterion 2 rejects all proposed IO sets.

In Fig. 2.5, the number of IO-sets which pass one of the two criteria at a certain frequency is depicted. Inequality (2.1) is evaluated for 200 frequency points which are logarithmically divided between 0.1 rad/s and 50 rad/s (ω_S). So, at each frequency point a subset of “viable” IO sets is isolated from the original set of 192 IO sets. From this figure, it is concluded that by application of Criterion 2, a considerably larger number of non-viable IO sets is eliminated.

In fact, IO sets are only viable if they pass the selection criterion for *all* frequencies below ω_S . In order to obtain the subset of viable IO sets, the following is done. Starting at $\omega = 0.1$, a particular subset of IO sets is accepted. This subset in turn is put to the test (2.1) at the next discrete frequency point. In Fig. 2.6, the number of IO sets passing the criterion for the *underlying* frequencies is depicted. Continuing for increasing frequencies, the number of IO sets which is still accepted is non-increasing. At ω_S , those IO sets remain, which pass the test for all frequencies of interest. For Criterion 2, they are listed in Table 2.3.

By applying Criterion 2, the overall set of candidates has been reduced to a more “manageable” subset of IO sets. The ultimate selection of an IO set could, *e.g.*, be performed by

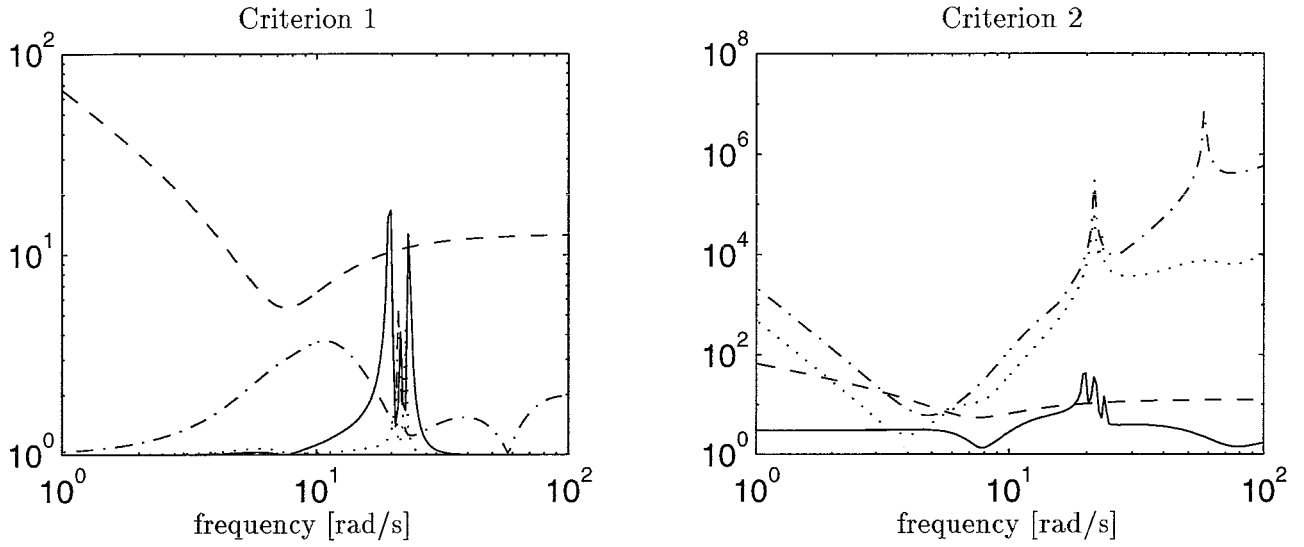


Figure 2.4: Difference between Criterion 1 and Criterion 2: $y_1 y_2 y_3$ (—), $y_1 y_3 y_4$ (---), $y_1 y_3 y_5$ (··) and evaluation bound (-.-)

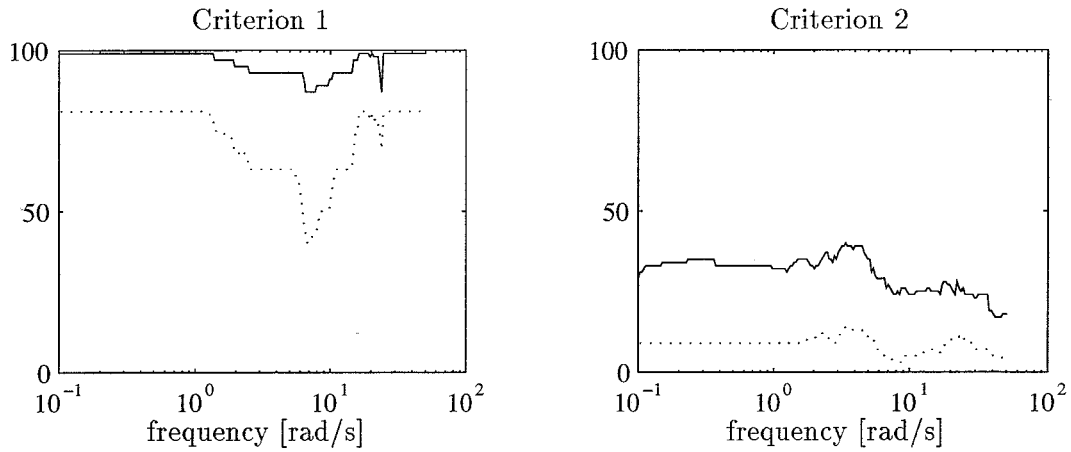


Figure 2.5: Number of candidate IO sets which pass the criteria *at a particular* frequency: 2×2 sets (—), 3×3 sets (··)

set number	2×2 IO sets	set number	3×3 IO sets
1	$y_4 y_5 / u_1 u_2$	7	$y_4 y_5 y_6 / u_1 u_2 u_3$
2	$y_4 y_6 / u_1 u_3$	8	$y_7 y_8 y_9 / u_1 u_2 u_3$
3	$y_5 y_6 / u_2 u_3$		
4	$y_7 y_8 / u_1 u_2$		
5	$y_7 y_9 / u_1 u_3$		
6	$y_8 y_9 / u_2 u_3$		

Table 2.3: IO sets which are accepted

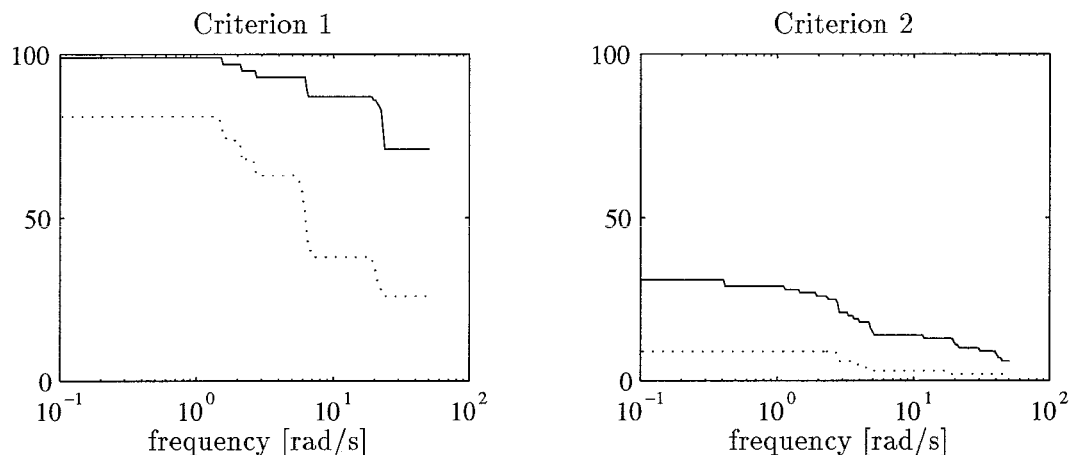


Figure 2.6: Number of candidate IO sets which pass the criteria for the *underlying* frequencies: 2×2 sets (-), 3×3 sets ($\cdot\cdot$)

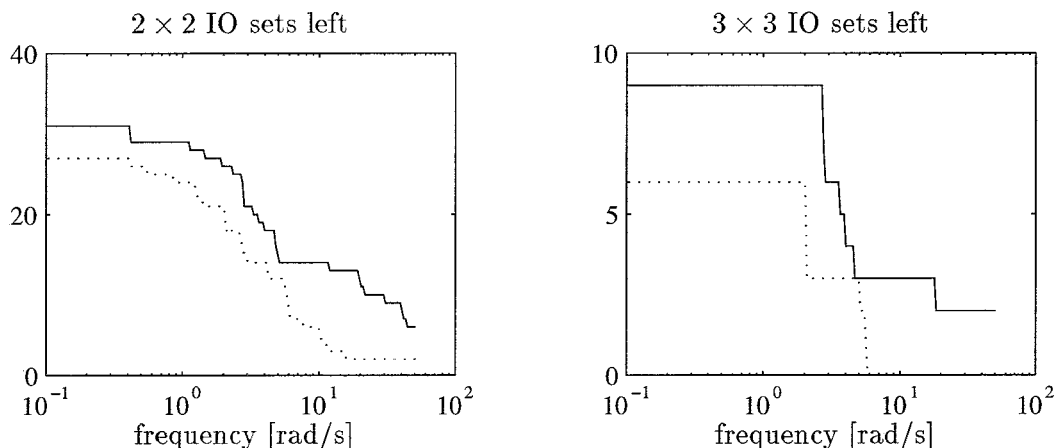


Figure 2.7: Number of IO sets passing Criterion 2 for the underlying frequencies applying δ_{ra} (-) and $2.5\delta_{ra}$ ($\cdot\cdot$)

designing controllers for each candidate, followed by an assessment of the closed-loop behavior. Alternatively, further screening could be performed, *e.g.*, by applying different sensitivity specifications or a different uncertainty bound, or by studying the condition numbers of the accepted IO sets in more detail.

One way to artificially *reduce* the number of accepted IO sets is to use a more conservative uncertainty bound, see Fig. 2.7. It is evident that if the relative additive uncertainty bound is larger, an equal or smaller number of IO sets pass the selection criterion at each frequency. This could of course be predicted from inequality (2.1). For $2.5\delta_{ra}$, the 3×3 IO sets are all eliminated, while 2×2 IO sets no. 1 and no. 4 (Table 2.3) are the only ones accepted. Another way to eliminate more IO sets is to raise ω_S . For example, by applying δ_{ra} and $\omega_S=100$ rad/s, 2×2 IO sets no. 1 till 4 and 3×3 IO set no. 7 are the only ones still accepted.

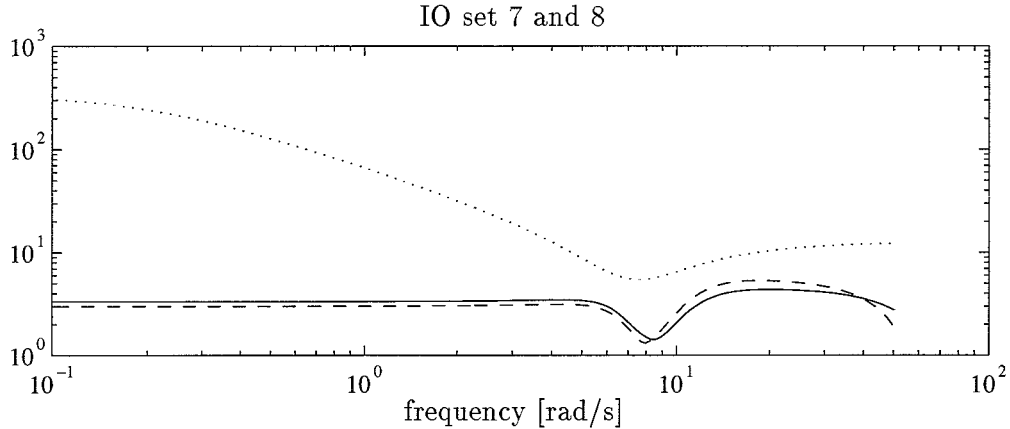


Figure 2.8: Condition numbers of the 3×3 accepted IO sets (set no. 7 (-), set no. 8 (- -)) and evaluation bound $1/(\delta_{ra}(1 - \sigma_S))$ (· ·)

The quality of the IO sets in Table 2.3 can also be assessed by comparing their condition numbers with the bound which it has to stay below. In Fig. 2.8, this is illustrated for the accepted 3×3 IO sets. Desirably, the condition number is small, since this will tolerate *larger* modeling errors and *smaller* sensitivity specifications. From Fig. 2.8 it is concluded that IO set no. 7 and 8 do not differ significantly; IO set no. 7 seems better for frequencies larger than 8 rad/s, while IO set no. 8 is slightly better for frequencies below 8 rad/s. Since the condition number of IO set no. 7 shows the least peaking, this one might be termed “best”.

In Fig. 2.9, the condition numbers for the accepted 2×2 IO sets and the evaluation bound are depicted. Since the condition number of IO set no. 1 shows the least peaking, this one is the best with regard to its ability to satisfy selection criterion (2.1).

Summarizing, IO sets no. 1 and no. 7 seem to offer the best prospects for robust stability and nominal closed-loop sensitivity, since the evaluation bound is easiest satisfied. Note that in both cases it is recommended to measure the vertical axle accelerations. Also note, that the measurements for each IO set in Table 2.3 are always of the *same type*, *i.e.*, only combinations of either vertical axle accelerations or vertical chassis accelerations occur. A sound physical explanation for these two facts is lacking at the moment.

Finally, it is emphasized once more, that in order to make a definitive choice for an IO set, it is best to design controllers for the most “promising” accepted candidates, followed by an assessment of the closed-loop behavior. This is however beyond the scope of this report.

2.3 Discussion

In this section, the IO selection method suggested in [3] has been illustrated for a practical example. In order to apply the criterion, an uncertainty bound δ_{ra} and specifications for the

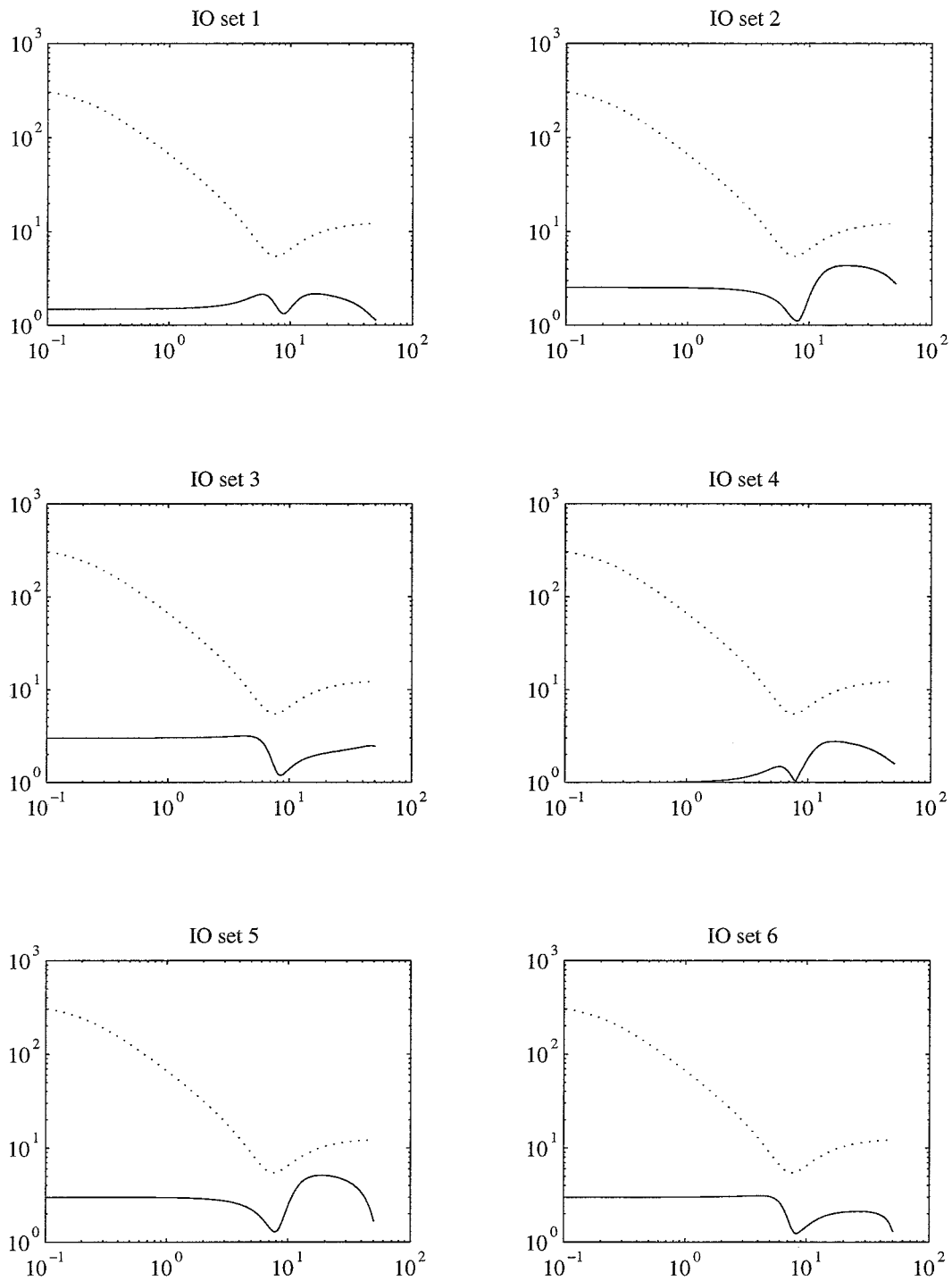


Figure 2.9: Condition numbers of the accepted 2×2 IO sets (-) and evaluation bound $1/(\delta_{ra}(1 - \sigma_S))$ (..)

nominal closed-loop sensitivity (ω_S, σ_S) have to be formulated. A major disadvantage of the method, is that these “design parameters” depend on the particular IO set under consideration, *i.e.*, distinct IO sets may both call for a different uncertainty bound and a different sensitivity specification (“performance specification”). However, due to the large number of candidate IO sets it is infeasible to derive uncertainty bounds and formulate sensitivity specifications for each candidate individually. Instead, they are formulated once and assumed to be representative for all candidate IO sets.

A related drawback of the IO selection method is the following. Although *a priori* nothing can be said about the value of $\kappa(A)$ compared to $\kappa(A^*)$, with A a sub-matrix of A^* , the tendency is, that $\kappa(A^*) > \kappa(A)$: computing condition numbers for 10,000 randomly generated 3×3 matrices, the mean condition number was 223, while for a 2×2 sub-matrix the mean condition number was 32. This may explain the fact that the number of 3×3 IO sets rejected is relatively large compared to the number of 2×2 sets rejected. The 1×1 IO sets with condition number 1 (smallest possible), *all* pass the selection criterion for the particular evaluation bound. Since it is noted that for *lower* dimensional subsystems the relative additive uncertainty $\bar{\sigma}(\Delta)/\bar{\sigma}(P_0)$ tends to be *larger* than for higher dimensional subsystems (see Fig. 2.2), it’s expected that formulating the uncertainty bound (and sensitivity specifications) for each candidate IO set individually yields a more effective, yet time-consuming, IO selection method.

Since a useful IO set can only be expected if a physically meaningful uncertainty bound is used, a frequency-dependent δ_{ra} has been derived for a particular choice of modeling errors. From the above it is clear that this bound may be conservative for particular IO sets, since it is designed to account for uncertainties in *all* candidate 2×2 and 3×3 IO sets. It has been illustrated that a more conservative uncertainty bound will eliminate a larger number of candidates (the same can be achieved by imposing tighter performance specifications, *e.g.*, by raising ω_S). In the examples discussed in [3], no attempt is made to derive a δ_{ra} which accounts for uncertainties occurring in practice. Instead, it is purely used as a design parameter to affect the number of IO sets that is rejected.

It has been shown that the difference in the number of IO sets which is rejected by Criterion 1 and Criterion 2 respectively may be substantial. Criterion 1 is only useful for *initial* screening of a large number of candidates. For this reason, the motivation for the introduction of Criterion 1 in [3] is doubtful: in order to obtain the subset of viable IO sets, Criterion 2 must be applied anyway, and moreover, there seems to be no computational advantage of Criterion 1 over Criterion 2.

Chapter 3

Control Configuration Selection

The procedure for Control Configuration (CC) selection is summarized in [5, Section 4.9]. For the sake of completeness, the main result will be repeated here.

The key idea behind CC selection is, that the performance degradation (in $y!$) of the nominal system in Fig. 1.2 must be restricted. In a centralized control system, each input u is determined by feedback from all measurements y , *i.e.*, full information exchange takes place. In a decentralized control system there is only a limited information flow through the controller, by which the performance may suffer. The following theorem is proven in [3]:

Suppose P is a square Finite Dimensional Linear Time Invariant (FDLTI) *nominal* plant with its measurements and manipulations partitioned such that:

$$P = [P_{ij}] = \begin{bmatrix} -P_{11} & \dots & -P_{1k} \\ \vdots & \ddots & \vdots \\ P_{k1} & \dots & P_{kk} \end{bmatrix}$$

Under these assumptions, there exists a FDLTI controller $C = \text{block diag}[C_{11}, \dots, C_{kk}]$ which achieves

1. $\bar{\sigma}[(T - \bar{T})\bar{T}^{-1}] \leq d_T$, and
2. $\bar{\sigma}(\bar{T}) \leq \sigma_{\bar{T}}$, $\sigma_{\bar{T}} < 1 \forall \omega \geq \omega_{\bar{T}}$

only if:

$$\frac{(1 - \sigma_{\bar{T}})\bar{\sigma}(V)}{1 + (1 - \sigma_{\bar{T}})\bar{\sigma}(V)} \leq d_T \forall \omega \geq \omega_{\bar{T}} \quad (3.1)$$

where:

- $V = (P - \bar{P})P^{-1}$ with $\bar{P} = \text{block diag}[P_{11}, \dots, P_{kk}]$

- d_T is the specified *maximum allowable* cross-feed performance degradation
- $T = PC(I + PC)^{-1}$ is the nominal output complementary sensitivity function
- $\bar{T} = \bar{P}C(I + \bar{P}C)^{-1}$ is the nominal output complementary sensitivity function of the associated block diagonal system
- $\sigma_{\bar{T}}$ and $\omega_{\bar{T}}$ specify the closed-loop bandwidth of the block diagonal system.

In the above, $\bar{\sigma}[(T - \bar{T})\bar{T}^{-1}]$ is introduced as a measure for Cross-Feed Performance Degradation (CFPD). It represents the “difference” between T and \bar{T} , relative to the ideal performance in \bar{T} . So, the closed-loop performance of P with the decentralized controller C is contrasted with that of the associated block diagonal system \bar{P} with C . If the off-diagonal blocks of P were not present and a decentralized controller with the same block structure were employed, cross-feed would not take place, and each of the subsystems P_{ii} could be controlled independently. The performance of the block diagonal system, composed of *independent* subsystems, is now considered “ideal”, which the real system’s performance should approximate. Note, that in case a centralized controller is used, there is no CFPD, since $\bar{P} = P$.

Inequality (3.1), which will be referred to as “Criterion 2”, is a necessary condition for low CFPD (provision 1), together with a specification for ideal performance (provision 2). Candidate configurations for which the CFPD is larger than maximally allowed, *i.e.*, larger than d_T , are rejected.

In [3], the scaling-dependence of $\bar{\sigma}(V)$ is the motivation to introduce the scaling-independent quantity $|\bar{\Psi}|_{max} = \max_i |\bar{\Psi}_i|$. It is the maximum absolute value complementary partial row sum of $\Lambda(P)$, for the configuration corresponding to \bar{P} ; $\bar{\Psi}_i$ is the sum of the RGA elements on the i -th row lying outside the diagonal block, see, *e.g.*, [5, Section 4.9]. In [3], it is shown that a new criterion for CC selection is created if $|\bar{\Psi}|_{max}$ is substituted for $\bar{\sigma}(V)$:

$$\frac{(1 - \sigma_{\bar{T}})|\bar{\Psi}|_{max}}{1 + (1 - \sigma_{\bar{T}})|\bar{\Psi}|_{max}} \leq d_T \quad \forall \omega \geq \omega_{\bar{T}} \quad (3.2)$$

The modified criterion (3.2) is scaling-independent and will be referred to as “Criterion 1”. Since $|\bar{\Psi}|_{max} \leq \bar{\sigma}(V)$, it provides a *weaker* necessary condition for low CFPD than Criterion 2 (3.1), by which more candidate configurations will pass.

Note, that Criterion 1 has a computational advantage over Criterion 2: for a particular IO set, the RGA needs to be calculated only once, since $|\bar{\Psi}|_{max}$ can simply be obtained by re-arranging rows and columns and imposing the corresponding configuration in the RGA (result from an algebraic property of the RGA, see, *e.g.*, [5, Section 4.4]). These operations are basically simpler than re-computing $\bar{\sigma}(V)$ for each candidate configuration. So, Criterion 1 may computationally be more *efficient*, though possibly less *effective*.

block structure	number of distinct configurations
{2,1}	9
{1,1,1}	6

Table 3.1: Number of candidate control configurations

configuration no.	block structure	configuration
1a	{2,1}	$[y_4 \ y_5] y_6 / [u_1 \ u_2] u_3$
2a	{2,1}	$[y_4 \ y_6] y_5 / [u_1 \ u_3] u_2$
3a	{2,1}	$[y_5 \ y_6] y_4 / [u_2 \ u_3] u_1$
4a	{1,1,1}	$y_4 \ y_5 \ y_6 / u_1 \ u_2 \ u_3$

Table 3.2: Accepted control configurations for IO set no. 7

3.1 Results

The selection of decentralized control configurations will be focussed on the 3×3 IO set $y_4 \ y_5 \ y_6 / u_1 \ u_2 \ u_3$, which seems to offer the best prospects for achieving robust stability. The selection will be performed with $\sigma_{\bar{T}} = \frac{1}{2}\sqrt{2}$, *i.e.*, $\bar{\sigma}(\bar{T})$ is specified to lie below the -3dB level for all frequencies ω greater than $\omega_{\bar{T}}$. For this specific example, $\omega_{\bar{T}}$ is fixed at 5 rad/s, in order to achieve robustness to uncertainties above $\omega_{\bar{T}}$, see Fig. 2.2. Note, that $\omega_{\bar{T}}$ is much smaller than $\omega_S=50$ rad/s, which was used for IO selection. This implies that both S and T are specified to be small in the frequency range between 5 and 50 rad/s. Since $S + T = I$, it's expected that a controller for which both specifications are achieved is very hard to design. However, for the purpose of CSD, imposing such overly demanding design specifications seems justified, since it will at least eliminate those candidates which offer “no prospects at all”.

From a 3×3 IO set, 15 distinct decentralized control configurations can be generated: 9 configurations consisting of one 2×2 block and one 1×1 block (denoted {2,1}), and 6 fully decentralized configurations consisting of three 1×1 blocks (denoted {1,1,1}), see Table 3.1.

Evaluation of the candidate control configurations will be performed in the region between $\omega_{\bar{T}}$ and 1000 rad/s. The difference in strength between Criterion 1 and Criterion 2 is illustrated by Fig. 3.1, in which the number of candidate configurations which pass the *underlying* frequencies for Criterion 1 or Criterion 2, is depicted. By setting $d_T=0.25$, all candidates pass Criterion 1, while four {2,1} and two {1,1,1} candidate configurations pass Criterion 2. If d_T is reduced to 0.15, the number of configurations passing is equal and constant for the whole frequency range of interest for both Criterion 1 and Criterion 2: the configurations which pass the criteria are listed in Table 3.2. Note that these configurations all correspond to “co-located” sensors and actuators, *i.e.*, measurement and manipulation are located “in the same place”.

To make possible a better comparison of the four configurations in Table 3.2, the corresponding CFPD quantities measures will be studied in detail. In Fig. 3.2, the left hand side of (3.1) is plotted for the {2,1} and the {1,1,1} configurations respectively. Obviously, configuration $[y_4 \ y_5] y_6 / [u_1 \ u_2] u_3$ (no. 1a) is the best, in the sense that the CFPD is smallest. For the

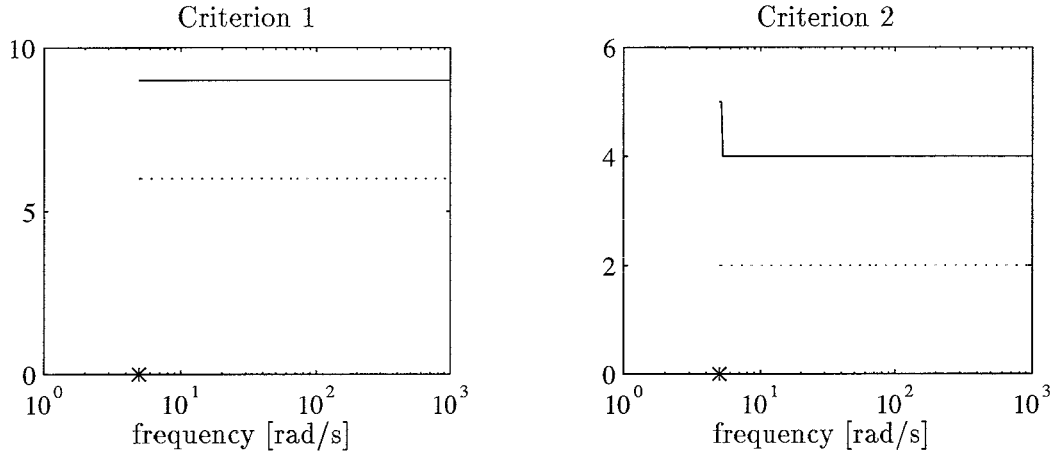


Figure 3.1: Number of configurations which pass the criteria for the *underlying* frequencies: $\{2,1\}$ (—), $\{1,1,1\}$ (··)

configuration no.	block structure	configuration
1b	$\{2,1\}$	$[y_7 \ y_8] \ y_9 / [u_1 \ u_2] \ u_3$
2b	$\{2,1\}$	$[y_7 \ y_9] \ y_8 / [u_1 \ u_3] \ u_2$
3b	$\{2,1\}$	$[y_8 \ y_9] \ y_7 / [u_2 \ u_3] \ u_1$
4b	$\{1,1,1\}$	$y_7 \ y_8 \ y_9 / u_1 \ u_2 \ u_3$

Table 3.3: Accepted control configurations for IO set no. 8

frequency range of interest, it is less than 7%. As a consequence, the performance with this configuration is expected to be only slightly worse than in case the centralized configuration $[y_4 \ y_5 \ y_6] / [u_1 \ u_2 \ u_3]$ is used.

If CC selection is performed for IO set no. 8 instead of no. 7, the configurations in Table 3.3 are accepted. Note that these configurations are the same as the ones in Table 3.2 if y_7 , y_8 and y_9 are replaced by y_4 , y_5 and y_6 respectively. Comparing CFPD for configuration no. 1a and no. 1b, it is concluded that the latter may be preferable, if *peaking* of the CFPD measure is the basis for quality assessment. So, performing CC selection for the bests IO set only, may not give the “optimal” control structure. It is illustrated, that although in Section 2.2 IO set no. 7 is preferred over IO set no. 8, the best configuration for IO set no. 7 may be “worse” than the best configuration for set no. 8. It is concluded, that in order to find the best controller structure, IO and CC selection are better not performed independently.

Suppose configuration no. 1a is used for design of a decentralized controller C with diagonal blocks C_{11} and C_{22} . The associated block diagonal system is denoted $\bar{P} = \text{block diag}[P_{11}, P_{22}]$, where P_{11} corresponds with the 2×2 transfer function matrix relating inputs $[u_1 \ u_2]$ to outputs $[y_4 \ y_5]$, and P_{22} corresponds with the transfer function between u_3 and y_6 . The design of C_{11} is based on P_{11} , while the design of C_{22} is based on P_{22} , *i.e.*, the controller for the active suspension of the tractor on the one hand and for the semitrailer on the other hand are designed independently. Note however, that this does *not* imply that if, *e.g.*, a different type of semitrailer or an unloaded one is used, controller C_{11} need not be re-designed. A different

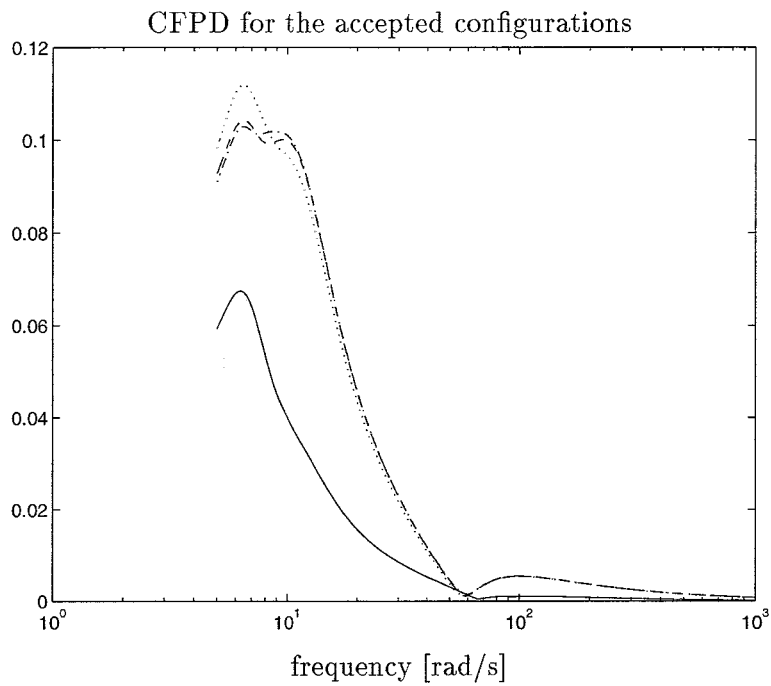


Figure 3.2: CFPD quantity for the most promising configurations in Table 3.2: no. 1a (-), no. 2a (\cdots), no. 3a (--), no. 4a (- \cdot)

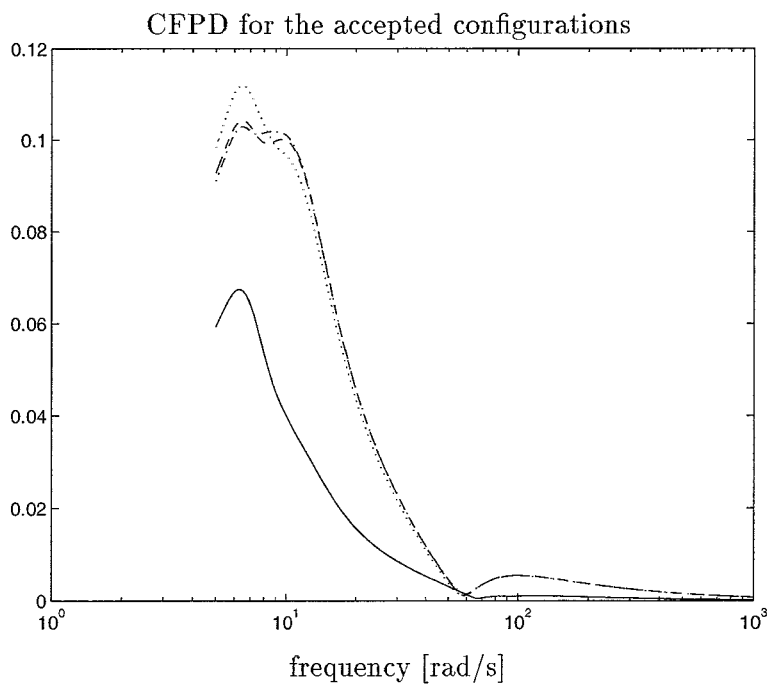


Figure 3.3: CFPD quantity for the most promising configurations in Table 3.3: no. 1b (-), no. 2b (\cdots), no. 3b (--), no. 4b (- \cdot)

semitrailer will not only cause changes in P_{22} , but in P_{11} as well. Therefore, both C_{11} and C_{22} may have to be re-designed.

In practice, the situation may occur that the tractor has to pull a semitrailer which is not actively suspended. Such a situation will cause problems in case the centralized configuration is used, since u_1 and u_2 need information on y_6 , which is not present. Provided the system remains stable if control loop y_6/u_3 is out of service (“closed-loop integrity” must be guaranteed, see, *e.g.*, [5, Section 4.10]), a decentralized controller based on configuration no. 1a seems more appropriate for practical application. Furthermore, the situation will occur that the tractor travels on its own. The centralized controller is expected to fail, while the decentralized controller is expected to work well, provided that it is robust to the changes in P_{11} , which are due to absence of the semitrailer.

Finally, it is remarked that the ultimate selection of the controller configuration should be performed in the context of controller design. The candidates in Table 3.2 and Table 3.3 may serve as a manageable basis of configurations for which this can be performed.

3.2 Discussion

The CC selection method proposed in [3] has been illustrated for a 3×3 IO set. It is concluded that CC selection Criterion 2 is able to eliminate a larger number of candidates than Criterion 1. Furthermore, reducing the maximally allowable CFPD d_T will eliminate more candidates. A remaining question is, if a frequency dependent d_T will improve CC selection. It is doubtful if the particular CC selection procedure is meaningful for frequencies far above ω_T , since performance is usually important below and just above the bandwidth. For this reason, it seems difficult to formulate a physically meaningful d_T .

After the complete set of candidate configurations has been reduced to a smaller subset of configurations which pass condition (3.1), more detailed studies of the associated frequency dependent CFPD’s can be performed to assess the quality of the accepted configurations. Alternatively, the quality of the accepted configurations may be assessed by controller design and closed-loop control system evaluation.

Bibliography

- [1] Okko Bosgra and Huibert Kwakernaak, “Design methods for control systems”, lecture notes from the Dutch Graduate Network on Systems and Control, spring term 1993-1994
- [2] Rudolf Huisman, “A controller and observer for active suspensions with preview”, PhD thesis, Eindhoven University of Technology, 1994
- [3] Deborah Edwards Reeves, “A comprehensive approach to control configuration design for complex systems”, PhD thesis, Georgia Institute of Technology, 1991
- [4] Deborah Edwards Reeves, Carl Nett, and Yaman Arkun, “Control configuration design toolbox for use with MATLAB”, user’s guide, version 1.0, May 1991
- [5] Marc van de Wal, “Control structure design for dynamic systems: A review”, WFW report 94.084, Eindhoven University of Technology, September 1994